Biochemical Journal Immediate Publication. Published on 27 Apr 2015 as manuscript BJ20141455

Metabolomic profiling in liver of adiponectin knockout mice uncovers lysophospholipid metabolism as an important target of adiponectin action

Ying Liu[1], Sanjana Sen[1], Sivaporn Wannaiampikul[1,2], Rengasamy Palanivel[1], Ruby L.C. Hoo[3], Ruth Isserlin[4], Gary D.Bader[4], Rungsunn Tungtrongchitr[2], Yves Deshaies[5], Aimin Xu[3] and Gary Sweeney[1]

[1]Department of Biology, York University, Toronto, Canada,
[2]Department of Tropical Nutrition and Food Science, Mahidol University, Bangkok, Thailand,
[3]State Key Laboratory of Pharmaceutical Biotechnology, and Department of Medicine, University of Hong Kong,
[4]The Donnelly Centre, University of Toronto, Canada,
[5]Department of Medicine and Québec Heart & Lung Institute Research Centre, Université Laval, Québec City, Canada.

*Address for correspondence:
Department of Biology
York University
Toronto, M3J1P3
Ontario, Canada.
Tel: (1)416-736-2100 (ext.66635)
e-mail: gsweeney@yorku.ca

Keywords: Adiponectin, insulin, hepatic, knockout, high fat diet, lipid, phospholipase
Wordcount: 5,079
Short title: Adiponectin regulated hepatic metabolism

Abstract

Adiponectin mediates antidiabetic effects via increasing hepatic insulin sensitivity and direct metabolic effects. In this study we conducted a comprehensive and unbiased metabolomic profiling of liver tissue from adiponectin knockout (AdKO) mice, with and without adiponectin supplementation, fed high fat diet (HFD) to derive insight into the mechanisms and consequences of insulin resistance. Hepatic lipid accumulation and insulin resistance induced by HFD were reduced by adiponectin. HFD significantly altered levels of 147 metabolites and bioinformatic analysis indicated that one of the most striking changes was the profile of increased lysophospholipids. These changes were largely corrected by adiponectin, at least in part via direct regulation of phospholipase A_2 (PLA_2) as palmitate-induced PLA_2 activation was attenuated by adiponectin in primary hepatocytes. Notable decreases in several glycerolipids after HFD were reversed by adiponectin which also corrected elevations in several diacylglycerol and ceramide species. Our data also indicate that stimulation of ω-oxidation of fatty acids by HFD is enhanced by adiponectin. In conclusion, this metabolomic profiling approach in AdKO mice identified important targets of adiponectin action, including PLA_2 to regulate lysophospholipid metabolism and ω-oxidation of fatty acids.

Introduction

Adiponectin, now well established as a potent anti-diabetic hormone [1, 2], is one of the most abundant circulating proteins in normal individuals but levels are reduced in individuals with obesity and diabetes [3]. Under normal conditions the 30 kDa adiponectin gene product undergoes posttranslational modifications and oligomerization to form trimers, hexamers and higher molecular weight oligomers prior to secretion. The latter are thought to be the most physiologically active forms of adiponectin and mediate potent anti-diabetic effects via numerous mechanisms. These include direct regulation of substrate metabolism, improved insulin sensitivity and anti-inflammatory actions. Adiponectin mediates these effects via at least two adiponectin receptor (AdipoR) isoforms and subsequent signaling mediated via their direct binding partner APPL1 and downstream targets including AMPK [4]. The anti-diabetic effects of adiponectin also encompass actions on various target tissues, in particular liver [5-8] and skeletal muscle [9-16].

Although previous work has conclusively established that adiponectin exerts beneficial metabolic effects by enhancing hepatic insulin sensitivity, we still do not fully understand the precise biochemical changes that occur. We recently examined metabolomic profiles of skeletal muscle samples from AdKO mice subjected to HFD with or without adiponectin replenishment [9]. Hyperinsulinemic-euglycemic clamp studies confirmed exaggerated insulin resistance in AdKO mice fed HFD which was corrected by adiponectin administration. Metabolomics data established important changes in response to HFD and we documented a signature of relatively normalized muscle metabolism across multiple metabolic pathways in response to adiponectin [9].

In the current study we conducted a comprehensive analysis of metabolomic profiles in liver of AdKO mice after HFD feeding to discover the major lipid metabolic pathways targeted by adiponectin action. Our aims were to characterize changes in peripheral metabolism, hepatic steatosis and insulin sensitivity in these mice and using metabolomic profiling to both confirm studies using alternative approaches in the existing literature and extend them to uncover novel targets of adiponectin action.

Experimental:

Animal Model: Male AdKO mice, kindly provided by Dr Y. Matsuzawa [17], on a C57BL6 background and littermates were routinely bred and genotyped in-house prior to being allocated to experimental groups. Animal facilities met the guidelines of the Canadian Council on Animal Care and all protocols used were approved by the Animal Care Committee, York University. Male adiponectin knock-out (AdKO) mice at 6 weeks of age were fed either regular chow or 60% high fat diet (HFD) for up to 6 weeks. HFD mice were given either saline or full length recombinant Ad at 3μg per gram of body weight, twice a day (9:00am and 6:00pm) via intraperitoneal injection, for an additional 2 weeks as previously described [9]. Prior to sacrifice, animals were deprived of food for 5-6 hours, and then subjected to hyperinsulinemic-euglycemic clamp. Insulin stimulation was administered as a 4 unit/kg body weight bolus via tail vein injection, 15 minutes after which liver tissues were harvested and snap frozen in liquid nitrogen. Serum samples were also collected and stored at -80°C.

In vitro studies in cultured cells: Primary mouse hepatocytes were isolated and cultured exactly as previously described [18]. HepG2 cells were generously provided by Dr. K. Adeli (University of Toronto) and were maintained as previously described [19]. Once confluent, cells were seeded onto culture plates in 2% FBS media 24 hours prior to treatment and treated as indicated in figure legends and additional methods below.

Western blot analysis: Small amounts of snap-frozen liver tissue were cut, crushed using a mortar and pestle, collected in Eppendorf tubes and homogenized in lysis buffer containing 0.1% NP-40, 30 mM Hepes pH7.4, 2.5 mM EGTA, 3 mM EDTA, 70 mM KCl, 20 mM beta-glycerophosphate, 20 mM NaF, 1 mM sodium orthovanadate, 200 μM PMSF, 1 μM pepstatin A, 10 μM E64, 1 μM leupeptin. HepG2 cells were lysed, essentially as previously described [10], with buffer containing Tris-HCl (pH 6.8, 0.5M), 10% SDS, 15% glycerol, 1 μM leupeptin, 200 μM PMSF, 10 μM E64, 1 mM sodium orthovanadate and 100 μM EDTA. Protein concentration of all samples was determined using the Pierce BCA Protein Assay kit (ThermoScientific Inc, Rockford) as per manufacturer's instructions and 30 μg total protein resolved by SDS-PAGE and transferred to PVDF membranes. Primary antibodies were diluted 1:1000 in a solution of 1 part 3% BSA and 2 parts 1X Wash Buffer (6.067g Tris base and 8.766g NaCl in ddH_2O) with 1 ml Tween and 1 ml NP-40. Immunodetection of proteins was visualized using enhancement chemiluminescence kit (Perkin Elmer) according to the manufacturer's instructions.

Triglyceride quantification: Total tissue triglyceride content was analyzed by a colorimetric Triglyceride Quantification kit purchased from Biovision (Mountain View, CA) according to manufacturer's instructions.

PCR analysis and array: Liver tissue samples were crushed to powder in liquid nitrogen, total RNA was extracted using TRIzol reagent (Invitrogen Life Technologies, Burlington, ON) and cleaning performed using RNeasy Mini Kit from Qiagen (Toronto, ON). cDNAs were synthesized by reverse transcription with 1 μg total RNA using RT^2 First-Strand cDNA Synthesis Kit from Qiagen (Toronto, ON). cDNA and RT^2 qPCR master mix solutions were aliquoted into 96-well plates pre-coated with primer sequences encoding various genes involved in fatty acid metabolism (Qiagen, Toronto, ON). Genes were normalized to several housekeeping genes including GAPDH, β-actin, and heat shock protein 90-α (HSP90α). Cycling conditions consisted of an initial denaturation step at 95°C for 3 min followed by 40 cycles at 95°C for 30s/ primer specific annealing temperatures 55-58°C for 30 s / 72°C for 30 s, the final extension was conducted at 72°C for 5 mins. Additional RT-PCR was performed using DyNAmo HS F-410L SYBR Green qPCR Kit (ThermoScientific). cDNA was produced using 0.25 μl Oligo dT (Sigma), 0.12 μl Random primers, 1 μl of dNTP, 2 μl of 5x First Strand Buffer (Invitrogen)

and 1μl D TT (Invitrogen) and 5.33 μl of nuclease-free water and incubated at 42°C for 2 mins. 0.3 μl of Reverse transcriptase supermix (Invitrogen) was added to each PCR tube and incubated at 42°C for 75 mins and at 94°C for 5 mins. The resulting cDNA was diluted 10 times in nuclease-free water prior to its use in the qPCR step. For qPCR, 10 ml of the F-410 (ThermoScientific) mastermix, 25 pmol of forward and reverse primers and 4 μl of the diluted cDNA and 4 μl of ddH_2O were added into new PCR tubes. Initial denaturation was conducted at 95°C for 15 mins, further denaturation was conducted at 94°C for 30 s / 57°C for 30 s / 72°C for 30 s for 40 cycles. The final extension was performed at 72°C for 5 mins and a melting curve created from 56°C to 95°C, reading every 1°C which was held for 1 sec. The qPCR product was recorded and c(t) values were collected on the Opticon Monitor 3 Software. The following sequences were used in qPCR experiments. Phospholipase A1 (captures all the splice variants X1-3): (fwd)GGCTCATCCTAACCCACAGT, (rev)ACACGCAGGCTATTTTCAGG; Phospholipase A2 (intracellular (cytosolic) group IVB): (fwd) GAGGTTGCTGCTGGTGATG, (rev)AGTCTGATGGGGTGTGTCG.

Phospholipase A_2 activity assay: Primary rat hepatocytes were isolated from male Wistar rats (180-250g) with collagenase perfusion as described above and previously [18], and seeded into 6-well culture dishes. Cells were then grown in DMEM medium with 1% serum treated without or with different concentrations of recombinant full length adiponectin for 8 hours, followed by treatment with palmitate (PA, 300 mM) or vehicle (lipid-free BSA) for 4 hours. The cells were harvested and intracellular activity of PLA_2 was measured with EnzChek® Phospholipase A_2 Assay Kit (Invitrogen).

Metabolomic and bioinformatic analysis: Global biochemical profiles were determined in liver as fee for service by Metabolon Inc. as previously described [9]. Scaled (to have a median of 1) metabolite expression values were used for further analysis. Two scenarios, comparing HFD vs Chow and HFD+Ad vs HFD, were analyzed to find pathways enriched with differentially expressed metabolites. Each sample was classified in terms of design type (i.e HFD vs Chow or HFD_Ad vs HFD). Metabolite expression samples in conjunction with the defined design type was then analyzed using GlobalANCOVA [20], which constructs a general linear model consisting of expression data and group the sample belongs to (i.e. HFD or Chow) compared to a model without the groups defined for each pathway to assess the significance of the grouping for the given set of metabolites. P-values were calculated using globalAncova's permutation-based method with 1000 perumutations and genesets were only examined if there were at least 3 metabolites associated with it. Pathway sets were collated from two sources: pathways defined by Metabolon Inc. and supplied in the original dataset from Metabolon and pathways from the MetaboAnalyst [21] website http://www.msea.ca/MSEA/faces/Resources.jsp.

GlobalANCOVA was performed on each pathway set to assess its significance. P-values were corrected using Benjamini Hochberg correction in R [22]. Resulting enrichments were formatted and visualized as a network in the Cytoscape network analysis and visualization software [23] using the Enrichment Map App [24] retaining only enrichments with *P*-value < 0.005 and FDR < 0.05. Nodes represent enriched pathways, and edges the metabolite overlap between two pathways. Only nodes that shared at least 30% of their metabolites were connected (calculated using Overlap coefficient > 0.3).

Since the GlobalANCOVA test gives no indication which direction (i.e. up or down regulated) the enriched pathway is altered, to better aid visualization of the enrichments for each pathway we calculated the ratio of significant up regulated genes to significant down regulated genes. In our data presentation, pathways with more up regulated genes are coloured red in the enrichment map visualization, pathways with more down regulated genes are blue and those that have equal amounts of up and down (or have no significantly altered genes) are white.

Histological analysis: Liver tissues were fixed prior to embedding in paraffin and for cryosections, tissues were cryoprotected in 30% sucrose for 24 hours prior to embedding in OCT compound and freezing in liquid nitrogen (N_2). Cryosections were cut at 7 μm and confocal images were quantified using ImageJ software. For hemotoxylin and eosin staining (Sigma), 5 μm paraffin sections of liver tissues were used. Slides were placed in oven (55°C) for 10 mins, deparaffinised in xylene twice for 15 minutes, rehydrated by placing in dilutions of ethanol ranging from 100% to 70%. Slides were then immersed in distilled water. Nuclei were stained by dipping slides in hematoxylin for 1 minute. Slides were rinsed in water and excess hematoxylin was removed with 1% hydrochloric acid in 70% ethanol then transferred to water. Slides were then dipped several times in Eosin, rinsed and dehydrated with ethanol (from 95% - 100%) and finally immersed in xylene. Stock solutions of oil red O (Fluka Chemica) were prepared using 0.5 g of oil red O and 100ml of isopropanol. The working solutions contained 30 ml of stock solution diluted in 20 ml of distilled water. Slides were incubated in coplin jars with Oil Red O working solution for 15 mins then rinsed with isopropanol followed by hemotoxylin staining 5 times and washed with distilled water.

Statistical analysis: All data were calculated as means ± SEM and further analyzed using nonparametric one-way ANOVA or two-way ANOVA with Tukey post-hoc test. Differences were considered statistically significant at $P< 0.05$.

Results

Hemotoxylin and eosin staining to examine morphology of liver tissue showed an increase in the number and size of vacuoles after HFD (Fig 1A). These vacuoles were noticeably diminished in size and number in mice administered Ad (Fig 1A). Oil Red O staining of liver tissue sections demonstrated a clear increase in the number of lipid droplets in HFD fed compared to chow fed mice. Interestingly, the number of large lipid droplets was significantly reduced in mice administered Ad (Fig 1B). Quantitative analysis of triglycerides in these tissues confirmed the aforementioned observations as the liver of AdKO mice fed a HFD contained 4 times more triglyceride than chow-fed mice (Fig 1C). HFD fed mice treated for an additional 2 weeks with Ad demonstrated levels of triglyceride similar to that of chow fed mice (Fig 1C). Compared to their chow-fed littermates, AdKO mice fed HFD demonstrated significantly reduced levels of insulin stimulated phosphorylation of Akt on Thr308 and Ser473 (Fig 1D&E). In AdKO mice fed HFD that received Ad treatment, insulin-stimulated phosphorylation levels were similar to (T308) or exceeded (S473) those of mice fed the chow diet (Figs 1D&E).

A global view of the metabolomic dataset (Table 1) indicated that HFD significantly altered 147 metabolites in liver (48 elevated and 99 reduced). Superimposing Ad treatment on HFD fed mice significantly altered the amount of 76 metabolites in liver (53 elevated and 23 reduced). To determine a global picture of how metabolite pathways are affected by diet and Ad, pathway enrichment analysis was performed on the set of differentially expressed metabolites for HFD compared to Chow and for HFD+Ad compared to HFD. Results were visualized as an enrichment map network. To enable easier comparison between the two enrichment results, enriched pathways from both results are shown in each map, but pathways not enriched in a given comparison are represented as white nodes without labels (Fig 2). HFD vs. Chow was enriched in 43 pathways whereas HFD+Ad vs. HFD was enriched in 32 pathways (p-value <0.005 and FDR < 0.05) of which 22 were common to both. More than half of the altered pathways were common to both comparisons yet the direction of metabolite differential expression was opposite for all but three of the pathways with a predominant down regulation of pathways in HFD vs. Chow and an up regulation of corresponding pathways in HFD+Ad vs. HFD. There was a larger subset of pathways (21 in HFD vs. Chow as compared to 10 in HFD+Ad vs. HFD) unique to HFD vs. chow, thus indicating a set of pathways which were not influenced by the administration of adiponectin. We also performed analysis to highlight those pathways affected by adiponectin, or not (Fig 3).

Lipid analysis revealed that HFD fed ADKO mice displayed a significant increase in ceramides 14:0, 20:0, 18:0, 18:1, 16:0 in the liver (Sup Fig 1). While there was an apparent trend towards a decrease in these levels with the administration of Ad, only ceramides 20:0 and 18:0 were significantly decreased. The total levels of ceramides remained unaltered between groups (Sup Fig 1). Levels of sphinganine and sphingosine, precursors of the ceramide/sphingosine-1-phosphate pathway, were significantly elevated in HFD group compared to chow-fed mice and levels of these metabolites were significantly decreased in HFD group treated with Ad. End-products of the palmitoyl-sphingomyelin pathway were significantly increased in the group treated with Ad compared to the group fed HFD alone (Sup Fig 1). In HFD mice the total levels of diacylglycerols (DAGs) were upregulated. Specific types of DAGs, 16:0-18:0, 18:0-18:2, 18:1, 16:1 and 18:0-20:4 were similarly elevated in the HFD group. Tissue from mice administered Ad displayed significantly attenuated levels of DAG 18:0-18:2 and 18:0-20:4 (Sup Fig 1).

Analysis of metabolomic profiles using Global ANCOVA indicated significant changes in fatty acid metabolism in response to HFD (Fig 2) and that adiponectin treatment had distinct effects on reversing some of these changes (Fig 3). Specifically, we found that HFD elevated levels of numerous long chain fatty acids, however Ad did not have any significant impact on these

changes (Sup Fig 2). Similarly, HFD-induced elevations in essential fatty acids EPA, n3 DPA and DHA were not altered by Ad (Sup Fig 2). The decreased deoxycarnitine and 3-dehydrocarnitine levels caused by HFD were not altered by Ad (Sup Fig 1). However, Ad did counteract HFD-induced decreases in 13-HODE, 9-HODE, 16-hydroxypalmitate, hexadecanedioate and caproate (Sup Fig 2). Further analysis of changes related to fatty acid metabolism were performed using a PCR array of relevant enzymes. Fig 4A shows that the majority of changes in gene expression induced by HFD occurred in those involved in fatty acid catabolism, and also in transport. A heat map showing changes in expression of all genes analyzed is shown in Fig 4B with changes induced by HFD in left column and the subsequent effect of Ad shown in right column. The principal changes are highlighted in Fig 4C and these included HFD-induced increases in Pdk4, Acads, Slc27a1 and Slc27a4 which were reduced by Ad. In contrast, Ad reversed HFD-induced decreases in UCP3, Cs, Acot9, Acadsb, Ppa1, Slc27a6, FABP5, FABP4, Prkab1, Prkaa1, Oxct2a and LPL gene expression (Fig 4C).

Bioinformatic analysis indicated that striking changes were observed in the category of lysolipids (Fig 2). In particular, those belonging to the group of lyso-phosphocholine and some lyso-phosphoethanolamines were significantly increased by HFD and subsequently decreased in the Ad-treated groups (Fig 5A). Of note, significant changes in both 1 and 2-acyl-glycerophosphocholine/ethanolamine were observed. Glycerol-3-phosphate was decreased in HFD groups compared to chow fed. There were also no changes in the levels of glycerophosphocholine (Fig 5A). Precursors of phosphotidylethanolamine formation such as ethanolamine and phosphoethanolamine showed significant decreases in the HFD group and a subsequent increase in groups treated with Ad (Fig 5A).

Because lysophospholipid metabolism was a major target of HFD and Ad, we next examined alterations in relevant phospholipase enzyme expression and activity. The relative expression levels of PLA1 and PLA2 were similar, based upon C(t) values. HFD elicited a significant increase in hepatic expression of PLA_1 and this was reversed in animals treated with Ad (Fig 5B), while PLA_2 levels were apparently increased by HFD and reduced by Ad (Fig 5B). To examine if Ad directly regulated phospholipase enzyme activity we used primary hepatocytes treated ± palmitate (300mM) and ± Ad (2.5ug/ml and 10ug/ml). The activity of PLA_2 was significantly elevated by palmitate and adiponectin significantly reduced palmitate-induced PLA2 activity (Fig 5C).

Further metabolomic data analysis, focusing on metabolites in the superpathway of carbohydrate metabolism, showed a trend of suppression of various metabolites after HFD, with significant decreases in maltose, fucose, ribulose, 6-phosphogluconate, UDP-glucose, UDP-galactose, fructose/glucose 1,6-diphosphate and lactate (Sup Fig 3). There were fewer significant effects of Ad on metabolites in this class, although significant decreases in 2-phosphoglycerate and 3-phosphoglycerate were notable (Sup Fig 3). In addition, supplementary figures show specific changes observed in amino acids (Sup Fig 4) and other metabolites (Sup Fig 5).

Discussion

Histological analysis as well as determination of total TG levels clearly indicated that HFD induced hepatic steatosis in AdKO mice which, as expected, was associated with insulin resistance. These defects were corrected by replenishment of adiponectin, confirming the beneficial antisteatotic and insulin sensitizing actions of adiponectin in the liver. To probe the precise changes in metabolism occurring under these conditions we used a metabolomic profiling approach to both confirm established and gain insight into new targets of adiponectin action in liver. Metabolomics is powerful in that it provides unbiased datasets which can be analyzed to infer mechanistic information [25, 26]. For example, metabolomic studies of liver from mice or rats subjected to HFD have demonstrated significant diet induced changes in lysolipids, choline, fatty acids and associated intermediates and amino acids [27-29]. The global summary of our current analysis indicated that 48 of 341 metabolites were significantly elevated in liver of AdKO mice after 6 weeks of HFD whereas 99 were reduced. The impact of replenishing adiponectin in these mice was to elevate 53 and reduce 23 metabolite levels. More informative data was then extracted by analysis of metabolomic alterations based on super- and sub-pathway categorization.

The most striking changes were observed in the category of lysophospholipids with HFD-induced increases in many distinct species, including lysophosphatidylcholines and lysophosphatidylethanolamines. Our metabolomic analyses demonstrate that both isoforms of lysophospholipids (1-and 2-acylglycerophospholipid) are altered with HFD and reversed with adiponectin treatment. Increased hepatic lysophospholipids have been reported previously in db/db mice and implicated as a cause of insulin resistance [30]. Interestingly, plasma lysophosphatidylcholine levels are reduced in obesity and type 2 diabetes [31] and a recent study specifically identified circulating lysophosphatidylcholine levels as markers of metabolically benign nonalcoholic fatty liver [32]. Lysophospholipids are also of great interest as recent literature has demonstrated their functional roles beyond membrane structure and function, including impairment of insulin signaling independent of ceramide and DAG, increase in VLDL assembly and secretion, fibrosis and inflammation [30, 33, 34]. Phospholipases and lysoPL-AT, enzymes that coordinate the regulation of lysolipid levels, have been shown to moderate hepatic lipotoxicity, insulin resistance and fibrosis [30, 35, 36]. The altered lysophospholipid levels we observed in liver tissue are most likely a result of an imbalance between phospholipase and lysoPL-AT activity [37]. Ad is known to enhance phospholipase C signaling in skeletal muscle cells [38], however, regulation of phospholipases A/B, lysoPL-AT and lysolipid levels by Ad has not been shown previously. We focused on PLA_2 given recent evidence implicating gain or loss of function in inducing [39] or preventing [40, 41] hepatic insulin resistance, respectively. We showed that adiponectin attenuated fatty acid-induced PLA_2 activity in primary hepatocytes, establishing PLA_2 as a new target of adiponectin action.

We also presume that increased saturated lysophosphatidylcholine would be accompanied by the release of arachidonate and modified eicosanoid synthesis. An interesting observation in our dataset was the HFD-induced increase in both 9-hydroxy-10,12-octadecadienoic acid (9-HODE) and 13-hydroxy-9,11-octadecadienoic acid (13-HODE), which was reversed by adiponectin. These are hydroxy derivatives of unsaturated linoleic acid and major components of OX-LDL [42]. Accordingly, they are considered good markers of lipid peroxidation [43], have potentially important roles in atherosclerosis [44] and have been shown to act as endogenous activators of peroxisome proliferator-activated receptor gamma (PPARγ) in various cell types [42, 43, 45] which is in keeping with our dataset indicating increased lipid uptake. These actions could also be considered beneficial in terms of insulin sensitivity and anti-inflammation.

Various lipids play an integral role in metabolic complications of hepatic steatosis [46] and we observed an expected overall increase in ceramides and DAGs in HFD fed mouse liver [47]. Specifically, data showing increased levels of intermediates such as sphinganine and reduced amount of precursors including L-serine indicated that HFD induced de novo synthesis of ceramides (14:0, 20:0, 18:0, 18:1, 16:0) with less influence on the salvage pathway of ceramide synthesis inferred by no change in sphingomyelin [48]. Our data indicate that adiponectin selectively reduced the levels of specific ceramides (20:0 and 18:0) and this appeared to be a result of influence on de novo and salvage pathways of ceramide synthesis [48]. In contrast, although effectively corrected here in liver, HFD induced increases in ceramide levels were not significantly altered by adiponectin in skeletal muscle [9]. Adiponectin also selectively reduced specific DAGs (18:0-18:2 and 18:0-20:4) in liver compared to our recent findings that in skeletal muscle HFD increased 16:0–18:1, 18:1, and 18:0–18:2 DAG species, all of which were reduced by adiponectin [9]. The differential effects of adiponectin supplementation in liver and skeletal muscle suggest that adiponectin regulates lipid metabolism in a tissue specific manner.

The oxidation of long chain fatty acids can occur via β-oxidation or the alternate pathway of ω-oxidation [49]. It has recently been suggested that ω-oxidation may act as a rescue pathway to reduce the accumulation of FAs and subsequent lipotoxic effects of their accumulation [49]. In this pathway fatty acids, particularly VLCFAs, are hydroxylated at the ω-carbon to produce ω-hydroxy-fatty acids and finally carboxylated to form ω–dicarboxylates in liver microsomes. Our metabolomics profile demonstrated increased levels of the intermediate, 16-hydroxypalmitate, and byproduct, hexadecanedioate, of ω-oxidation [49]. Interestingly, adiponectin also increased both of these metabolites, suggesting that it may also upregulate ω-oxidation and that, depending on the prevailing physiological and cellular milieu, this can be beneficial.

Having established the altered profile of fatty acid metabolites we used a PCR array to detect changes in enzymes involved in fatty acid metabolism. First, we observed a decrease in pyrophosphatase, suggesting a decrease in energy demands [50]. This is congruent with the decrease in fatty acid oxidation after HFD. Acyl-CoA thioesterase and acyl-CoA dehydrogenase, enzymes involved in fatty acid β-oxidation and in the inhibition of lipogenesis were reduced, which further supports an increase in lipogenesis, and a decrease in fatty acid β-oxidation in HFD-fed AdKO mice. Adiponectin significantly increased levels of enzymes involved in fatty acid uptake and oxidation, including uncoupling protein UCP, citrate synthase, HSP90 alpha B1, FATP, 3-oxoacid coA transferase 2A, FABP and 2,4-dienoyl reductase 1. While an increase in fatty acid uptake with adiponectin treatment may seem to oppose the notion that adiponectin action is beneficial and reduces lipotoxicity, it is known that in the event of an increased systemic demand for fatty acid utilization, the liver takes up free fatty acids and increases oxidation while simultaneously breaking down stored triglycerides, packaging them as VLDLs and secreting them into the circulation [51]. Furthermore, this increased fatty acid uptake may be coupled to the increased ω-oxidation which we observed and described above.

Glucose metabolism across multiple metabolic routes was perturbed under HFD conditions. Known impacts of HFD induced insulin resistance on glucose metabolism in liver include elevated rates of gluconeogenesis and glycogen breakdown, even under hyperglycemic conditions [52]. In this study, HFD decreased levels of lactate and some amino acids which typically serve as precursors for gluconeogenesis, perhaps indicating elevated gluconeogenesis. Significantly lower levels for many intermediates of the TCA cycle support the notion of poor oxidative energy metabolism with HFD, consistent with glucose production by liver. Although adiponectin improves insulin sensitivity, the HFD-induced shifts in glycolytic/gluconeogenic pathway intermediates and changes in TCA cycle intermediates were not completely rectified by adiponectin

supplementation. Our findings that treatment with fAd for 2 weeks was unable to reverse all of the effects of the HFD in AdKO mice is consistent with our observation that glucose infusion rates in these mice were also only partially restored after fAd treatment for 2 weeks. Thus, we feel it is important to point out that a longer duration of adiponectin treatment could conceivably elicit greater, or different, effects and this remains to be tested.

In addition to the consideration of individual metabolites discussed above, we determined major changes in groups of metabolites and applied an established pathway analysis pipeline, most often used with gene expression data, to further analyse our metabolomics data. Briefly, in liver from HFD fed mice, predominant changes included decreased protein biosynthesis and fatty acid metabolism but marked increases in lysolipids and long chain fatty acids. This analysis confirmed that with the addition of adiponectin there was an increase in protein synthesis and fatty acid metabolism as well as a decrease in lysolipids. Although our pathway analysis provides a useful summary of our results at the systems level, some measured metabolites were not considered because they are not annotated to any pathway. A limitation of this approach is that a few metabolites were not annotated with Human Metabolite Database (HMDB) identifiers (~27%) which eliminated a large proportion of our metabolites from subsequent pathway analysis. Another limitation was that the Metabolon database consisted of annotations that are metabolite specific with only one annotation per metabolite. Metabolites belonging to multiple pathways are not specified leading to loss of information for metabolites that play a role in multiple pathways. Improved pathway annotations will improve metabolomics pathway analysis in the future. Nevertheless, this analysis rapidly identifies statistically significant changes in metabolic pathways and provides a useful comprehensive summary of our dataset.

In this study we have validated the HFD-induced development of insulin resistance and hepatic steatosis in AdKO mice and our metabolomics approach has proven useful in i) confirming established literature regarding changes in lipid metabolites such as ceramides and diacylglycerols in response to HFD and the ability of adiponectin to correct these and ii) uncovering novel targets of adiponectin action associated with lipid metabolism. The latter include the novel observation that upregulation of lysophospholipids in response to HFD may have contributed to the phenotypes of HFD-induced insulin resistance, impaired glucose tolerance and hypertriglyceridemia and that adiponectin-mediated reversal of these changes may occur partly via regulation of PLA_2 activity. The stimulation of ω-oxidation of fatty acids by adiponectin and the ability of adiponectin to reverse changes in 9-HODE and 13-HODE may also have previously uncharacterized implications in systemic metabolic dysfunction and resulting complications.

Acknowledgements

This work was supported by an operating grant from the Canadian Institutes of Health Research to GS, who is guarantor of this work. We also acknowledge HKU matching fund for State Key Laboratory of Pharmaceutical Biotechnology to AX and NRNB (U.S. National Institutes of Health, National Center for Research Resources grant number P41 GM103504) to GDB. SW received support from Royal Golden Jubilee Award (Thailand Research Fund). We acknowledge the expert advice from Dr David Brindley (University of Alberta) and Dr Dominic Ng (University of Toronto) on lipid metabolism data and experimental planning. No conflicts of interest are declared by the authors. Author contributions included experimental work (YL,SS,SW,PR,RLCH), intellectual input and study design (YL,SS,AX,GS), specific data analysis (RI,GB), writing and editing of the manuscript (YL,SS,RT,RI,GB,YD, AX,GS).

References

1 Turer, A. T. and Scherer, P. E. (2012) Adiponectin: mechanistic insights and clinical implications. Diabetologia. **55**, 2319-2326

2 Scheid, M. P. and Sweeney, G. (2013) Adiponectin signaling and changes in metabolic disease. Reviews in Endocrine and Metabolic Disorder **in press**

3 Liu, Y., Retnakaran, R., Hanley, A., Tungtrongchitr, R., Shaw, C. and Sweeney, G. (2007) Total and high molecular weight but not trimeric or hexameric forms of adiponectin correlate with markers of the metabolic syndrome and liver injury in Thai subjects. J Clin Endocrinol Metab. **92**, 4313-4318

4 Deepa, S. S. and Dong, L. Q. (2009) APPL1: role in adiponectin signaling and beyond. American journal of physiology. Endocrinology and metabolism. **296**, E22-36

5 Nawrocki, A. R., Rajala, M. W., Tomas, E., Pajvani, U. B., Saha, A. K., Trumbauer, M. E., Pang, Z., Chen, A. S., Ruderman, N. B., Chen, H., Rossetti, L. and Scherer, P. E. (2006) Mice lacking adiponectin show decreased hepatic insulin sensitivity and reduced responsiveness to peroxisome proliferator-activated receptor gamma agonists. J Biol Chem. **281**, 2654-2660

6 Berg, A. H., Combs, T. P., Du, X., Brownlee, M. and Scherer, P. E. (2001) The adipocyte-secreted protein Acrp30 enhances hepatic insulin action. Nat Med. **7**, 947-953

7 Combs, T. P., Berg, A. H., Obici, S., Scherer, P. E. and Rossetti, L. (2001) Endogenous glucose production is inhibited by the adipose-derived protein Acrp30. J Clin Invest. **108**, 1875-1881

8 Yamauchi, T., Kamon, J., Waki, H., Terauchi, Y., Kubota, N., Hara, K., Mori, Y., Ide, T., Murakami, K., Tsuboyama-Kasaoka, N., Ezaki, O., Akanuma, Y., Gavrilova, O., Vinson, C., Reitman, M. L., Kagechika, H., Shudo, K., Yoda, M., Nakano, Y., Tobe, K., Nagai, R., Kimura, S., Tomita, M., Froguel, P. and Kadowaki, T. (2001) The fat-derived hormone adiponectin reverses insulin resistance associated with both lipoatrophy and obesity. Nat Med. **7**, 941-946

9 Liu, Y., Turdi, S., Park, T., Morris, N. J., Deshaies, Y., Xu, A. and Sweeney, G. (2013) Adiponectin corrects high-fat diet-induced disturbances in muscle metabolomic profile and whole-body glucose homeostasis. Diabetes. **62**, 743-752

10 Liu, Y., Chewchuk, S., Lavigne, C., Brule, S., Pilon, G., Houde, V., Xu, A., Marette, A. and Sweeney, G. (2009) Functional significance of skeletal muscle adiponectin production, changes in animal models of obesity and diabetes, and regulation by rosiglitazone treatment. American journal of physiology. Endocrinology and metabolism. **297**, E657-664

11 Krause, M. P., Liu, Y., Vu, V., Chan, L., Xu, A., Riddell, M. C., Sweeney, G. and Hawke, T. J. (2008) Adiponectin is expressed by skeletal muscle fibers and influences muscle phenotype and function. Am J Physiol Cell Physiol. **295**, C203-212

12 Ceddia, R. B., Somwar, R., Maida, A., Fang, X., Bikopoulos, G. and Sweeney, G. (2005) Globular adiponectin increases GLUT4 translocation and glucose uptake but reduces glycogen synthesis in rat skeletal muscle cells. Diabetologia. **48**, 132-139

13 Vu, V., Liu, Y., Sen, S., Xu, A. and Sweeney, G. (2013) Delivery of adiponectin gene to skeletal muscle using ultrasound targeted microbubbles improves insulin sensitivity and whole body glucose homeostasis. American journal of physiology. Endocrinology and metabolism. **304**, E168-175

14 Vu, V., Bui, P., Eguchi, M., Xu, A. and Sweeney, G. (2013) Globular adiponectin induces LKB1/AMPK-dependent glucose uptake via actin cytoskeleton remodeling. J Mol Endocrinol. **51**, 155-165

15 Vu, V., Kim, W., Fang, X., Liu, Y. T., Xu, A. and Sweeney, G. (2007) Coculture with primary visceral rat adipocytes from control but not streptozotocin-induced diabetic animals increases glucose uptake in rat skeletal muscle cells: role of adiponectin. Endocrinology

16 Vu, V., Dadson, K., Odisho, T., Kim, W., Zhou, X., Thong, F. and Sweeney, G. (2011) Temporal analysis of mechanisms leading to stimulation of glucose uptake in skeletal muscle cells by an adipokine mixture derived from primary rat adipocytes. Int J Obes (Lond). **35**, 355-363

17 Maeda, N., Shimomura, I., Kishida, K., Nishizawa, H., Matsuda, M., Nagaretani, H., Furuyama, N., Kondo, H., Takahashi, M., Arita, Y., Komuro, R., Ouchi, N., Kihara, S., Tochino, Y., Okutomi, K., Horie, M., Takeda, S., Aoyama, T., Funahashi, T. and Matsuzawa, Y. (2002) Diet-induced insulin resistance in mice lacking adiponectin/ACRP30. Nat Med. **8**, 731-737

18 Cheng, K. K., Iglesias, M. A., Lam, K. S., Wang, Y., Sweeney, G., Zhu, W., Vanhoutte, P. M., Kraegen, E. W. and Xu, A. (2009) APPL1 potentiates insulin-mediated inhibition of hepatic glucose production and alleviates diabetes via Akt activation in mice. Cell Metab. **9**, 417-427

19 Qiu, W., Kohen-Avramoglu, R., Rashid-Kolvear, F., Au, C. S., Chong, T. M., Lewis, G. F., Trinh, D. K., Austin, R. C., Urade, R. and Adeli, K. (2004) Overexpression of the endoplasmic reticulum 60 protein ER-60 downregulates apoB100 secretion by inducing its intracellular degradation via a nonproteasomal pathway: evidence for an ER-60-mediated and pCMB-sensitive intracellular degradative pathway. Biochemistry. **43**, 4819-4831

20 Hummel, M., Meister, R. and Mansmann, U. (2008) GlobalANCOVA: exploration and assessment of gene group effects. Bioinformatics. **24**, 78-85

21 Xia, J. and Wishart, D. S. (2011) Web-based inference of biological patterns, functions and pathways from metabolomic data using MetaboAnalyst. Nature protocols. **6**, 743-760

22 Benjamini, Y. and Hochberg, Y. (1995) Controlling the false discovery rate: a practical and powerful approach to multiple testing. Journal of the Royal Statistical Society Series B. **57**, 289-300

23 Shannon, P., Markiel, A., Ozier, O., Baliga, N. S., Wang, J. T., Ramage, D., Amin, N., Schwikowski, B. and Ideker, T. (2003) Cytoscape: a software environment for integrated models of biomolecular interaction networks. Genome Res. **13**, 2498-2504

24 Merico, D., Isserlin, R., Stueker, O., Emili, A. and Bader, G. D. (2010) Enrichment map: a network-based method for gene-set enrichment visualization and interpretation. PLoS One. **5**, e13984

25 Patti, G. J., Yanes, O. and Siuzdak, G. (2012) Innovation: Metabolomics: the apogee of the omics trilogy. Nat Rev Mol Cell Biol. **13**, 263-269

26 Bain, J. R., Stevens, R. D., Wenner, B. R., Ilkayeva, O., Muoio, D. M. and Newgard, C. B. (2009) Metabolomics applied to diabetes research: moving from information to knowledge. Diabetes. **58**, 2429-2443

27 Kim, H. J., Kim, J. H., Noh, S., Hur, H. J., Sung, M. J., Hwang, J. T., Park, J. H., Yang, H. J., Kim, M. S., Kwon, D. Y. and Yoon, S. H. (2011) Metabolomic analysis of livers and serum from high-fat diet induced obese mice. J Proteome Res. **10**, 722-731

28 Bertram, H. C., Larsen, L. B., Chen, X. and Jeppesen, P. B. (2012) Impact of high-fat and high-carbohydrate diets on liver metabolism studied in a rat model with a systems biology approach. J Agric Food Chem. **60**, 676-684

29 Rubio-Aliaga, I., Roos, B., Sailer, M., McLoughlin, G. A., Boekschoten, M. V., van Erk, M., Bachmair, E. M., van Schothorst, E. M., Keijer, J., Coort, S. L., Evelo, C., Gibney, M. J., Daniel, H., Muller, M., Kleemann, R. and Brennan, L. (2011) Alterations in hepatic one-carbon metabolism and related pathways following a high-fat dietary intervention. Physiol Genomics. **43**, 408-416

30 Han, M. S., Lim, Y. M., Quan, W., Kim, J. R., Chung, K. W., Kang, M., Kim, S., Park, S. Y., Han, J. S., Park, S. Y., Cheon, H. G., Dal Rhee, S., Park, T. S. and Lee, M. S. (2011) Lysophosphatidylcholine as an effector of fatty acid-induced insulin resistance. J Lipid Res. **52**, 1234-1246

31 Barber, M. N., Risis, S., Yang, C., Meikle, P. J., Staples, M., Febbraio, M. A. and Bruce, C. R. (2012) Plasma lysophosphatidylcholine levels are reduced in obesity and type 2 diabetes. PLoS One. **7**, e41456
32 Lehmann, R., Franken, H., Dammeier, S., Rosenbaum, L., Kantartzis, K., Peter, A., Zell, A., Adam, P., Li, J., Xu, G., Konigsrainer, A., Machann, J., Schick, F., Hrabe de Angelis, M., Schwab, M., Staiger, H., Schleicher, E., Gastaldelli, A., Fritsche, A., Haring, H. U. and Stefan, N. (2013) Circulating lysophosphatidylcholines are markers of a metabolically benign nonalcoholic fatty liver. Diabetes Care. **36**, 2331-2338
33 Pyne, N. J., Dubois, G. and Pyne, S. (2013) Role of sphingosine 1-phosphate and lysophosphatidic acid in fibrosis. Biochim Biophys Acta. **1831**, 228-238
34 Morris, A. J., Panchatcharam, M., Cheng, H. Y., Federico, L., Fulkerson, Z., Selim, S., Miriyala, S., Escalante-Alcalde, D. and Smyth, S. S. (2009) Regulation of blood and vascular cell function by bioactive lysophospholipids. J Thromb Haemost. **7 Suppl 1**, 38-43
35 Li, Z., Ding, T., Pan, X., Li, Y., Li, R., Sanders, P. E., Kuo, M. S., Hussain, M. M., Cao, G. and Jiang, X. C. (2012) Lysophosphatidylcholine acyltransferase 3 knockdown-mediated liver lysophosphatidylcholine accumulation promotes very low density lipoprotein production by enhancing microsomal triglyceride transfer protein expression. J Biol Chem. **287**, 20122-20131
36 Ishihara, K., Miyazaki, A., Nabe, T., Fushimi, H., Iriyama, N., Kanai, S., Sato, T., Uozumi, N., Shimizu, T. and Akiba, S. (2012) Group IVA phospholipase A2 participates in the progression of hepatic fibrosis. FASEB J. **26**, 4111-4121
37 Aloulou, A., Ali, Y. B., Bezzine, S., Gargouri, Y. and Gelb, M. H. (2012) Phospholipases: an overview. Methods Mol Biol. **861**, 63-85
38 Zhou, L., Deepa, S. S., Etzler, J. C., Ryu, J., Mao, X., Fang, Q., Liu, D. D., Torres, J. M., Jia, W., Lechleiter, J. D., Liu, F. and Dong, L. Q. (2009) Adiponectin activates AMP-activated protein kinase in muscle cells via APPL1/LKB1-dependent and phospholipase C/Ca2+/Ca2+/calmodulin-dependent protein kinase kinase-dependent pathways. J Biol Chem. **284**, 22426-22435
39 Hadad, N., Burgazliev, O., Elgazar-Carmon, V., Solomonov, Y., Wueest, S., Item, F., Konrad, D., Rudich, A. and Levy, R. (2013) Induction of cytosolic phospholipase a2alpha is required for adipose neutrophil infiltration and hepatic insulin resistance early in the course of high-fat feeding. Diabetes. **62**, 3053-3063
40 Iyer, A., Lim, J., Poudyal, H., Reid, R. C., Suen, J. Y., Webster, J., Prins, J. B., Whitehead, J. P., Fairlie, D. P. and Brown, L. (2012) An inhibitor of phospholipase A2 group IIA modulates adipocyte signaling and protects against diet-induced metabolic syndrome in rats. Diabetes. **61**, 2320-2329
41 Song, H., Wohltmann, M., Bao, S., Ladenson, J. H., Semenkovich, C. F. and Turk, J. (2010) Mice deficient in group VIB phospholipase A2 (iPLA2gamma) exhibit relative resistance to obesity and metabolic abnormalities induced by a Western diet. American journal of physiology. Endocrinology and metabolism. **298**, E1097-1114
42 Nagy, L., Tontonoz, P., Alvarez, J. G., Chen, H. and Evans, R. M. (1998) Oxidized LDL regulates macrophage gene expression through ligand activation of PPARgamma. Cell. **93**, 229-240
43 Negishi, M., Shimizu, H., Okada, S., Kuwabara, A., Okajima, F. and Mori, M. (2004) 9HODE stimulates cell proliferation and extracellular matrix synthesis in human mesangial cells via PPARgamma. Exp Biol Med (Maywood). **229**, 1053-1060
44 Vangaveti, V., Baune, B. T. and Kennedy, R. L. (2010) Hydroxyoctadecadienoic acids: novel regulators of macrophage differentiation and atherogenesis. Ther Adv Endocrinol Metab. **1**, 51-60
45 Itoh, T., Fairall, L., Amin, K., Inaba, Y., Szanto, A., Balint, B. L., Nagy, L., Yamamoto, K. and Schwabe, J. W. (2008) Structural basis for the activation of PPARgamma by oxidized fatty acids. Nat Struct Mol Biol. **15**, 924-931

46 Bikman, B. T. and Summers, S. A. (2011) Sphingolipids and hepatic steatosis. Adv Exp Med Biol. **721**, 87-97
47 Turner, N., Kowalski, G. M., Leslie, S. J., Risis, S., Yang, C., Lee-Young, R. S., Babb, J. R., Meikle, P. J., Lancaster, G. I., Henstridge, D. C., White, P. J., Kraegen, E. W., Marette, A., Cooney, G. J., Febbraio, M. A. and Bruce, C. R. (2013) Distinct patterns of tissue-specific lipid accumulation during the induction of insulin resistance in mice by high-fat feeding. Diabetologia. **56**, 1638-1648
48 Grosch, S., Schiffmann, S. and Geisslinger, G. (2012) Chain length-specific properties of ceramides. Prog Lipid Res. **51**, 50-62
49 Wanders, R. J., Komen, J. and Kemp, S. (2011) Fatty acid omega-oxidation as a rescue pathway for fatty acid oxidation disorders in humans. FEBS J. **278**, 182-194
50 Kajander, T., Kellosalo, J. and Goldman, A. (2013) Inorganic pyrophosphatases: one substrate, three mechanisms. FEBS Lett. **587**, 1863-1869
51 Liu, M., Chung, S., Shelness, G. S. and Parks, J. S. (2012) Hepatic ABCA1 and VLDL triglyceride production. Biochim Biophys Acta. **1821**, 770-777
52 Hoo, R. L., Lee, I. P., Zhou, M., Wong, J. Y., Hui, X., Xu, A. and Lam, K. S. (2013) Pharmacological inhibition of adipocyte fatty acid binding protein alleviates both acute liver injury and non-alcoholic steatohepatitis in mice. J Hepatol. **58**, 358-364

Table 1. *Global profiling of 341 metabolites.* Welch's Two Sample *t*-tests were used to determine whether the means of two groups are different where $P \leq 0.05$ was taken as significant and *P* value trend of $0.05 < P < 0.10$ identified biochemicals approaching significance.

Welch's Two Sample t-Test Liver Tissue	**HF CHOW**	**HF + fAD CHOW**	**HF + fAD HF**
Total number of biochemicals with $p \leq 0.05$	**147**	**102**	**76**
Biochemicals (↑ ↓)	**48 | 99**	**39 | 63**	**53 | 23**
Total number of biochemicals with $0.05 < p < 0.10$	23	27	35
Biochemicals (↑ ↓)	8 | 15	13 | 14	26 | 9

Figure Legends:

Figure 1: Lipid accumulation and insulin signalling in liver. AdKO mice fed either regular chow or 60% HFD for 6 weeks. HFD mice received an additional 2-week adiponectin or saline treatment at the dosage of 3 μg/g body wt via IP injection. Liver tissues were then collected 15mins after 4U/kg insulin stimulation for later analysis. A) Hemotoxylin and Eosin staining of paraffin-embedded cross-sections of liver tissues (200X). B) TG content in liver tissues. C) Oil Red O staining of cryosections of liver tissues (400X). D&E) Representative western blot and analysis of insulin stimulated Akt at phosphorylation sites Ser473 and Thr308. Scale bars for IHC= 200□μm. Data represent mean ± SEM. * Significant difference between Chow vs HF group, # Significant difference between saline-treated vs adiponectin-treated HFD groups. *# P<0.05, **##P<0.01, ***###P<0.001

Figure 2: Bioinformatics analysis of differentially expressed pathways. Enriched pathways in HFD vs. Chow (A) and HFD+Ad vs. HFD (B) data. Pathways are represented by nodes in the network. Size of the nodes directly correlates to the number of metabolites annotated to a pathway. Node colour indicates direction of metabolite expression causing the significant enrichment, where red is up-regulation, blue is down-regulation and white indicates there are equal numbers of up and down regulated metabolites (or no change). Edges (lines) represent known pathway crosstalk, defined by the number of metabolites shared between a pair of pathways (as calculated using the overlap coefficient < 0.3). To enable easier comparison between the two enrichment maps, all results were merged, but only the pathways relevant for a particular comparison are highlighted (colours and labels).

Figure 3: Bioinformatic analysis of pathways altered by adiponectin or not. HFD vs Chow enriched pathway network highlighting pathways rescued(A) and not rescued (B) by adiponectin. Enriched pathways in HFD vs Chow are annotated with node labels and colours indicating the direction of metabolite expression, where red is up-regulation, blue is down-regulated and white indicates there was no change. The transparency of the nodes was increased in (A) if it was a pathway not seen in the HFD fAD vs HFD enriched pathway set to highlight pathways (common to both HFD vs Chow and HFD fAD vs HFD) that were rescued by adiponectin. The transparency of the nodes was increased in (B) if it was a pathway found in HFD fAD vs HFD enriched pathway set to highlight pathways unique to HFD vs Chow and not rescued by adiponectin.

Figure 4: Quantitative PCR Array analysis of genes involved in fatty acid metabolism. AdKO mice fed either regular chow or 60% HFD for 6 weeks. HFD mice received an additional 2 weeks' adiponectin or saline treatment at the dosage of 3 μg/g body wt via IP injection. Liver tissues were then collected 5mins after 4U/kg insulin stimulation for later analysis. A) Effect of HFD on genes involved in fatty acid metabolism. B) Heat map revealed effect of HFD (left panel) and adiponectin (right panel) on genes involved in fatty acid metabolism C). List of genes involved in fatty acid metabolism that was significantly altered by HFD and significantly corrected by adiponectin treatment. Data represent fold change.

Figure 5: Metabolomic analysis of lysolipid species profiles and analysis of phospholipase activity. A) shows lysolipid metabolite changes in AdKO mice treated as described in figure 1. *Left panel:* fold change between Chow and HFD fed AdKO mice, *Right panel*: fold change between adiponectin- versus saline-treated HFD fed AdKO mice. Data represent mean ± SEM. Significant difference between Chow vs HF group, # Significant difference between saline-treated vs adiponectin-treated HFD group. *# P<0.05, **##P<0.01, ***###P<0.001. B) The hepatic mRNA expression of phospholipase A_1 (PLA_1) and A_2 (PLA_2) were analyzed in tissue samples from AdKO mouse groups matching data in A. C) Primary hepatocytes were isolated and treated ± palmitate or ± as described and the activity of PLA_2 was determined. Data represent mean ± SEM. * Significant difference between Chow vs HF group or control cell group, # Significant difference between saline-treated vs adiponectin-treated HFD groups. *# P<0.05, **##P<0.01, ***###P<0.001

Biochemical Journal Immediate Publication. Published on 27 Apr 2015 as manuscript BJ20141455

Figure 1

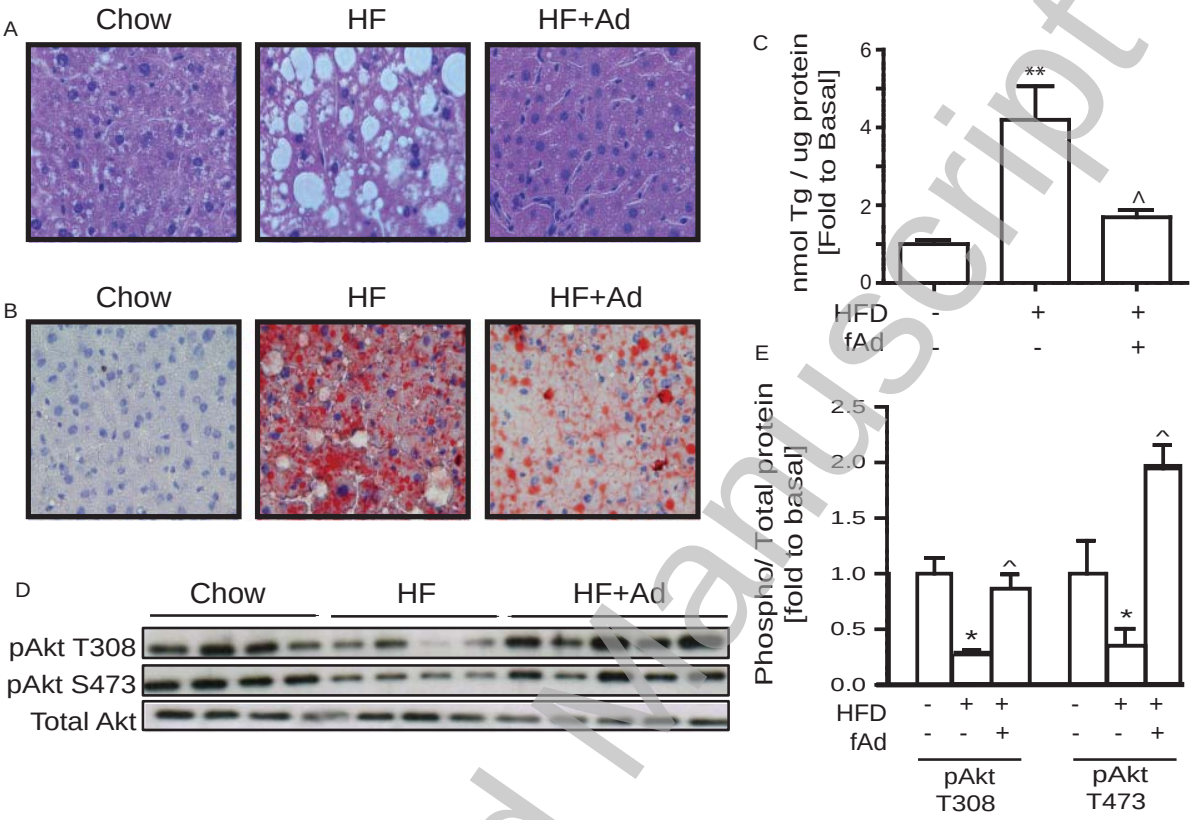

Biochemical Journal Immediate Publication. Published on 27 Apr 2015 as manuscript BJ20141455

Figure 2

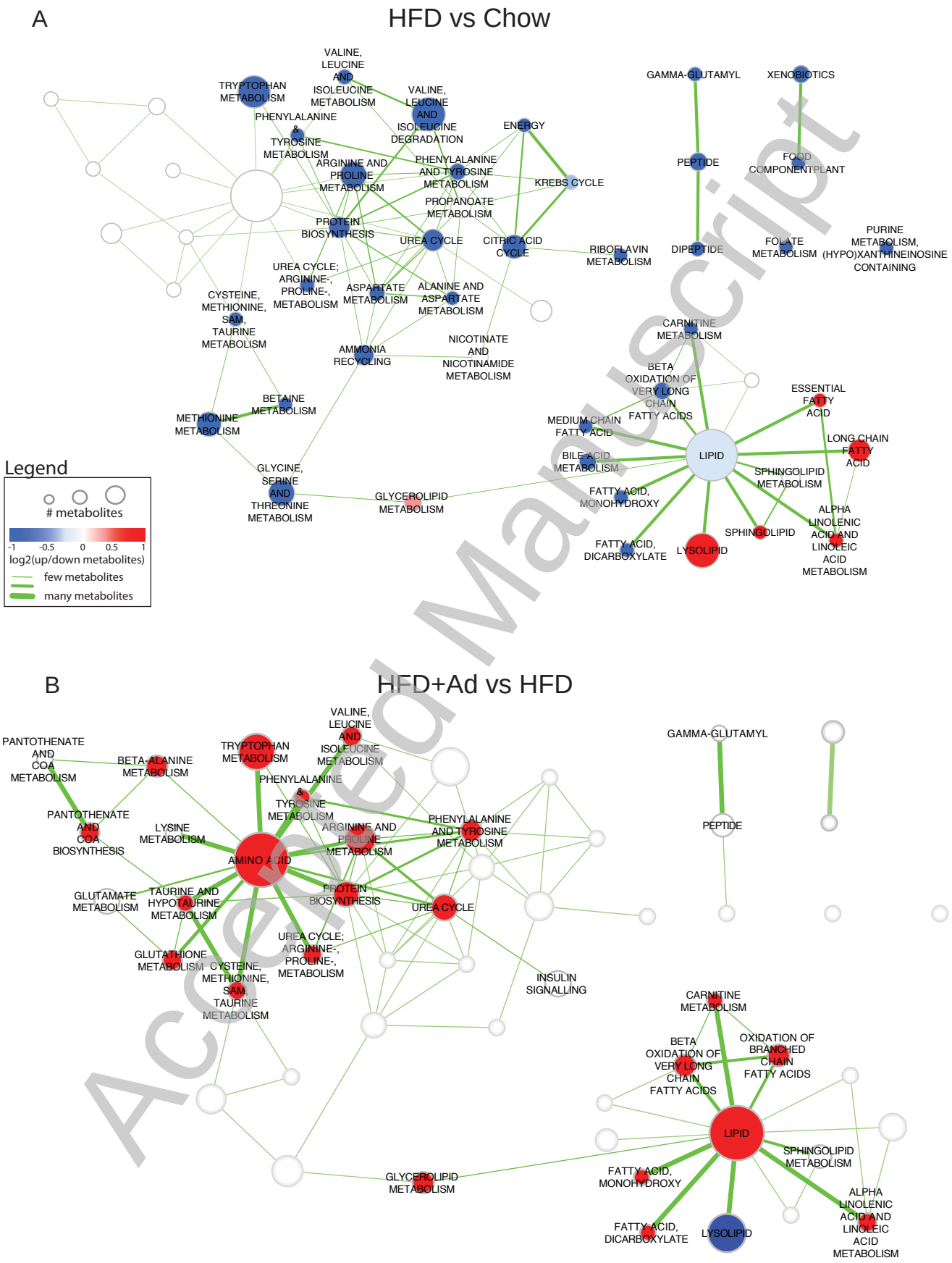

Biochemical Journal Immediate Publication. Published on 27 Apr 2015 as manuscript BJ20141455

Figure 3

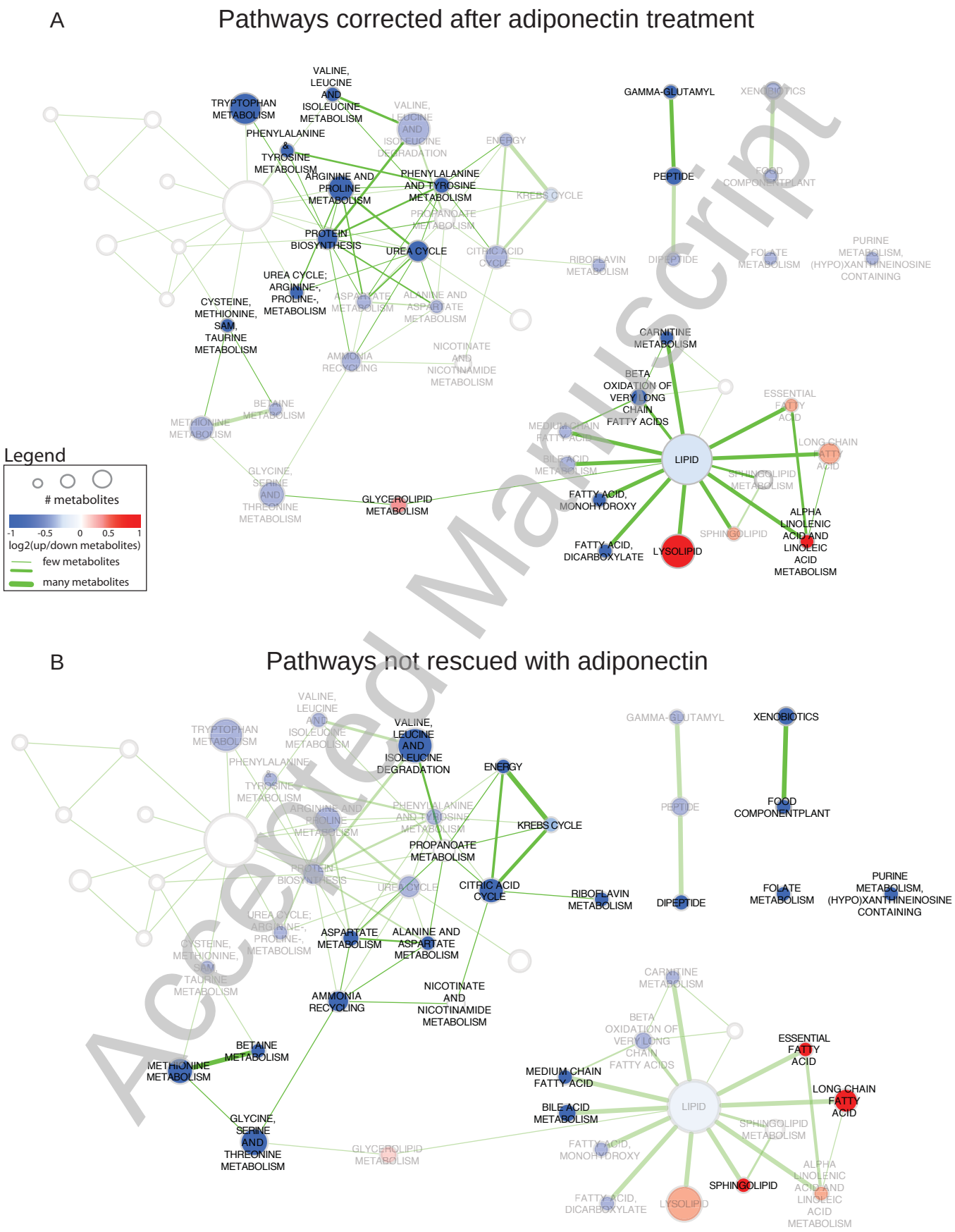

Biochemical Journal Immediate Publication. Published on 27 Apr 2015 as manuscript BJ20141455

Figure 4

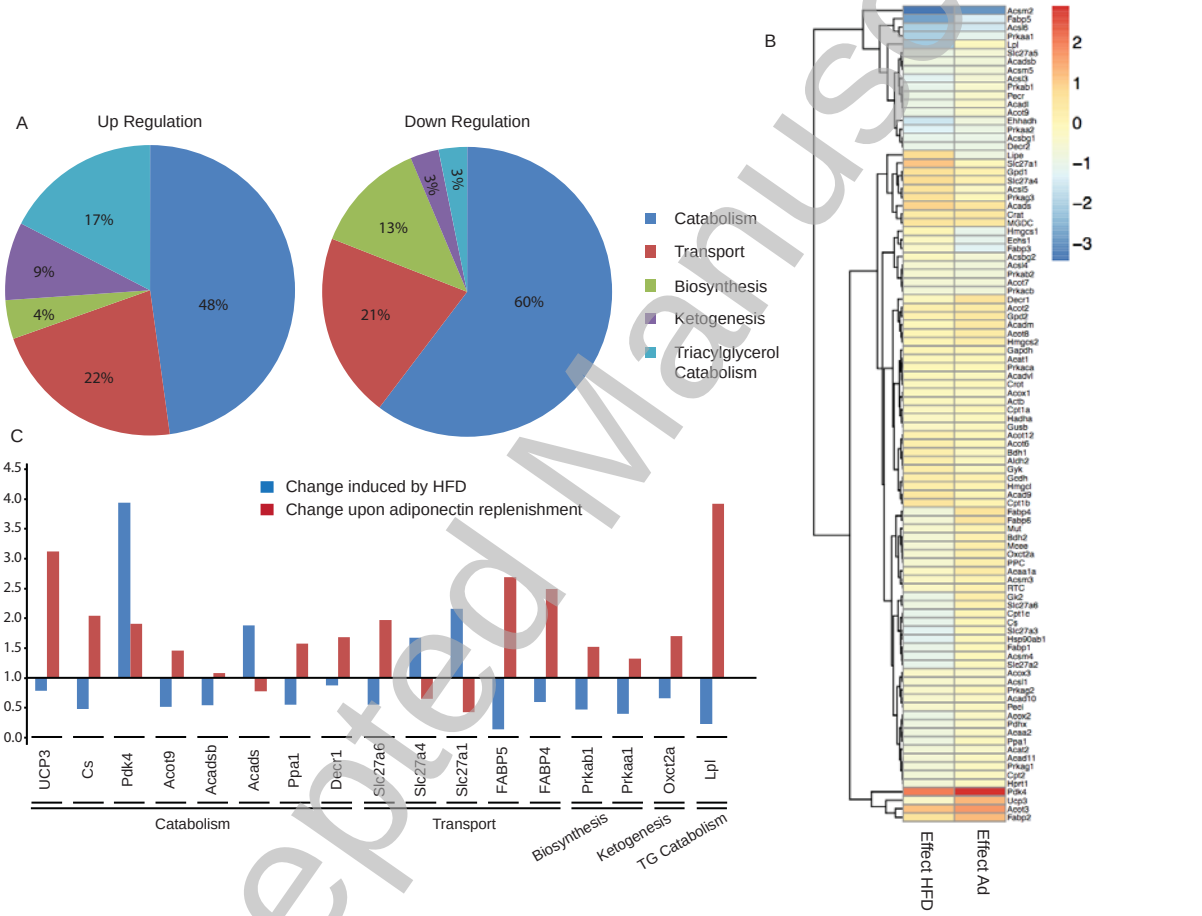

Figure 5